

MASTER

UCRL-87025
PREPRINT

CONF-8105103--2

Gold Transmission Gratings with
Submicrometer Periods and Thickness > 0.5 μ m

N. Ceglio, R. Price, A. Hawryluk, J. Melngailis and
H. Smith

This paper was prepared for submittal to the
16th Symposium Electron Ion and Photon Beam
Technology, Dallas, Texas, May 26-29, 1981

December, 1981

This is a preprint of a paper intended for publication in a journal or proceedings. Since changes may be made before publication, this preprint is made available with the understanding that it will not be cited or reproduced without the permission of the author.

Lawrence
Livermore
Laboratory

UCRL--87025

DE82 010065

⁷ Gold Transmission Gratings with
Submicrometer Periods and Thickness > 0.5 μ m

A. M. Hawryluk*

Department of Electrical Engineering and Computer Science
Massachusetts Institute of Technology
Cambridge, Massachusetts 02139

N. M. Ceglio** and Robert H. Price**

Lawrence Livermore National Laboratory
Livermore, California 94550

J. Melngailis* and Henry I. Smith*

Research Laboratory of Electronics
Massachusetts Institute of Technology
Cambridge, Massachusetts 02139

ABSTRACT

Gold gratings with spatial periods of 0.3 and 0.2 μ m have been fabricated in thicknesses of 0.6 and 0.25 μ m, respectively, and used in x-ray spectroscopy and spatial-period-division. Fabrication techniques included: holographic lithography, shadowing, x-ray lithography and gold microplating. Control of linewidth to tolerances of the order of 10 nm has been demonstrated for gratings of 0.2 μ m period. A high resolution imaging spectrometer, composed of a 2x Wolter x-ray microscope in conjunction with a gold transmission grating, was tested. At a wavelength of 0.69 nm a resolving power, $\lambda/\Delta\lambda$, of 200 was demonstrated. Resolution in this case was source size limited. Gratings of 99.5 nm period were exposed in PMMA by x-ray ($\lambda = 4.5$ nm) spatial-period-division.

* This work was sponsored by the Joint Services Electronics Program and the Defense Advanced Research Project Agency.

** Work performed under the auspices of the U.S. Department of Energy under contract No. W-7405-Eng-48.

I. INTRODUCTION

We have fabricated transmission gratings in thick gold with spatial periods of 0.3 and 0.2 μm and used the former for spectroscopy at 0.6-0.7 nm and the latter for spatial-period-division¹⁻³ with C_K x-rays (4.5 nm). The 0.3 μm period gratings had a gold thickness of 0.6 μm and thus the attenuation through the lines exceeded 10 dB for x-ray wavelengths above 0.8 nm,⁴ leading to a nearly uniform diffraction efficiency. At a wavelength of 0.69 nm the attenuation through 0.6 μm of gold is 8 dB. For x-ray spectroscopy, gratings should either be supported on a transmissive membrane or be "free standing". We have fabricated both types. The "free standing" gratings were held together by an integral coarse grid.

For spatial-period-division there are rather stringent requirements on the "parent mask". Attenuation through opaque regions should exceed about 25 dB and thus with the C_K x-ray (4.5 nm) a gold thickness greater than 200 nm is required.² Moreover, for "doubling" a parent mask of period p , the width of the transmissive portions ("slits") of the mask should be equal to or less than $p/4$.¹ We fabricated parent masks of period 199 nm in gold 250 nm thick with slit widths of 40 nm.

II. FABRICATION OF GRATINGS

The fabrication of the gratings began with holographic lithography. We used a He:Cd laser ($\lambda = 325$ nm) and a configuration in which spatial filters were the final elements in the two interferometer arms. As a result, the grating period increases as a function of distance from the center of the interference pattern. The spatial filters were positioned about 1/2 m from the substrate. Assuming spherical wavefronts, it is relatively easy to show that in the plane of the interferometer the spatial period increased by 1 part in 10^4 at distances of 5 and 7 mm from the pattern center for the 0.3 and 0.2 μm patterns respectively. This distortion can be made arbitrarily small by increasing the distance from the spatial filters to the substrate.

For the 0.3 μm period gratings, we exposed in ~ 50 nm thick AZ 1350J* photoresist on ~ 70 nm thick gold on ~ 1 μm thick polyimide on silicon wafers. The gold was then ion beam etched (Fig. 1) and a polyimide membrane x-ray mask was produced by epoxy bonding the polyimide to a ring and then chemically etching away the silicon substrate. This mask was then used to expose ~ 1 μm thick films of PMMA. To minimize line widening due to diffraction and penumbra, the x-ray mask was held in intimate contact with the PMMA by applying an electrostatic potential between the substrate and an aluminum film on the back side of the polyimide membrane. X-ray exposures were done using the C_k ($\lambda = 4.5$ nm) x-ray into PMMA over a plating base of 10 nm Au/10 nm chromium on a substrate which was either 0.5 μm thick polyimide on a Si wafer (for

*Shipley Co., Newton, MA

the case of membrane supported gratings) or a bare silicon wafer (for the case of free-standing gratings). After removing any resist residue between exposed lines with a O_2 plasma, gold microplating was carried out in a commercial solution (Sel-Rex BDT-510) at a temperature of 45°C and a solution pH of 8.5. A plating rate of 10 nm/min gave the best results. After plating, the PMMA was dissolved in chlorobenzene. Fig. 2a shows the PMMA after exposure and before microplating. Fig. 2b shows a completed gold diffraction grating.

For polyimide-membrane supported gratings, the silicon substrate behind the grating area was simply etched away chemically. Since polyimide absorbs strongly (i.e., $> 10 \text{ dB}/\mu\text{m}$) at wavelengths between 2.5 and 4.3 nm and beyond $\sim 7 \text{ nm}$, self-supported gratings are preferred for spectroscopy at these wavelengths. To accomplish this we photolithographically superimposed and microplated a coarse grid on top of the $0.3 \mu\text{m}$ grating. First a $0.5 \mu\text{m}$ thick layer of AZ 1350B* was spun over a $0.3 \mu\text{m}$ period, $0.45 \mu\text{m}$ thick, gold grating on a silicon substrate. Then a second layer of $3 \mu\text{m}$ thick AZ 1350J* resist was spun on. A $6 \mu\text{m}$ period grating was exposed perpendicular to the $0.3 \mu\text{m}$ period grating and a $160 \mu\text{m}$ period grating was exposed parallel to the $0.3 \mu\text{m}$ period grating. This grid was then electroplated to a thickness of $3 \mu\text{m}$. The linewidth-to-period ratios of the $6 \mu\text{m}$ and $160 \mu\text{m}$ period gratings were 5 to 8 and 1 to 8 respectively, so that $\sim 30\%$ of the area of the $0.3 \mu\text{m}$ period grating was unobstructed by the support grid. After plating, the resist was dissolved and the silicon behind the grating etched away.

*Shipley Co., Newton, MA

The 199 nm period gratings, with slits of 40 nm in gold 250 nm thick, were fabricated by a multistep process which differs somewhat from that described earlier.¹ Holographic lithography produced a grating pattern in ~ 50 nm AZ 1350J* resist over 10 nm thick Cr over 20 nm thick Si₃N₄ on (100) Si wafers. Chemical etching of the Cr, followed by reactive ion etching of the Si₃N₄, followed by KOH anisotropic chemical etching⁵ produced a sawtooth-profile structure in the (100) silicon. A polyimide mold taken from this structure was then epoxy bonded to a ring and obliquely shadowed with tungsten to produce an x-ray mask with 40 nm wide lines on 199 nm centers.⁶ This was then x-ray replicated in 150 nm thick PMMA over a 1 μ m thick polyimide membrane on a Si wafer followed by liftoff of 10 nm Cr and 50 nm Au. After etching away the silicon, this yielded an x-ray mask with ~ 40 nm wide slits in gold 60 nm thick. This "polarity-reversed" mask was then replicated into 250 nm thick PMMA over a 1 μ m thick polyimide membrane on a silicon wafer followed by liftoff of 10 nm Cr/60 nm Au to yield a third x-ray mask having the same "polarity" as the original sawtooth mask but with much higher contrast (~ 8 db). This third mask was then used to expose ~ 40 nm wide lines, on 199 nm centers, in 250 nm thick PMMA over a gold plating base on polyimide over a silicon wafer. After gold plating to a thickness between 200 and 250 nm the final "parent mask" was epoxy bonded to a ring. Fig. 3 shows a mask made for spatial-period-division but which was sacrificed for microscopy.

III. X-RAY SPECTROSCOPY

To test the spectroscopic performance of our grating we used a Wolter 22x grazing incidence microscope⁷ and an electron bombarded tungsten anode source to provide narrow lines at 0.698, 0.676 and 0.609 nm, corresponding to the tungsten M_{α} , M_{β} , and M_{γ} respectively. The Wolter microscope has a spatial resolution of $\sim 1\mu\text{m}$. A $4\mu\text{m}$ thick gold foil with a pattern of apertures ranging from 6×9 to $2 \times 2\mu\text{m}$ was placed at the object plane of the Wolter microscope and back-lit by the tungsten source. By grazing incidence reflections off the hyperboloid and ellipsoidal surfaces of the microscope, the x-rays are focused onto the image plane located 6.6 m away. The gratings were placed, as depicted in Fig. 4, 5.92 m from the image plane. A rectangular area, 7 mm parallel and 0.3 mm perpendicular to the grating lines, was illuminated. In general, the $0.3\mu\text{m}$ period gratings were used for spectroscopy although a few experiments were done with $0.2\mu\text{m}$ period gratings. Fig. 5 shows the zeroth and 1st order diffracted images, as recorded in x-ray film. A microdensitometer trace of this film indicated a resolving power, $\lambda/\Delta\lambda$, of 200 at $\lambda = 0.69$ nm. This resolution is limited by the source size and not by distortion in our gratings, which we estimate to be $< 10^{-4}$ over the area illuminated by the x-rays, taking into account membrane distortion⁸ ($< 10^{-4}$) and the use of spherical wavefronts in the holographic lithography ($< 10^{-4}$ over the entire illuminated area). We measured a transmission diffraction efficiency (ratio of the energy in one first

order to the energy in the zeroth order) of 100% (\pm 10%) for the 0.3 μm period, 0.6 μm thick, gratings. For comparison, the theoretical efficiency of a grating with fully opaque lines should be 40%. The higher efficiency obtained experimentally can be accounted for by partial transmission and appropriate phase shift through the grating lines. Others⁹ have reported diffraction efficiencies of 16% for 0.42 μm period transmission gratings.

IV. SPATIAL-PERIOD-DIVISION

For spatial-period-division we used parent masks of 199 nm period with slits of \sim 40 nm width in gold 200 to 250 nm thick (see Fig. 3). The x-ray source was an electron bombarded carbon anode. The parent mask was held apart from a PMMA coated substrate by means of polyimide spacers, as described earlier.¹ Both fixed gap (4.3 μm) and variable gap (3-5 μm) spacers were used, and the openings in the polyimide spacers were 25 x 25 μm . As before, an electrostatic potential held the mask-spacer-substrate assembly together.

To eliminate problems due to penumbra or motion of the beam impingement point on the anode, a slit aperture was placed between the source and substrate, which gave an effective source size of \sim 1 x 2 mm. Source-to-substrate distance was 100 mm, and the source was operated at 6.0 kV and 30 ma. Fig. 6 shows a recent result, a 99.5 nm period grating exposed in PMMA. An exposure time of 140 hours was required. The increase, by a factor of 9 X, in the exposure time relative to our

initial spatial-period-division work can be accounted for by the different source operating parameters ($\sim 1.6 \text{ X}$), a thicker polyimide membrane and gold plating base ($\sim 2 \text{ X}$), the use of an aperture ($\sim 2 \text{ X}$) and more complete exposure ($\sim 1.5 \text{ X}$). Clearly, a brighter source, such as a synchrotron, and further improvements in techniques are required before x-ray spatial-period-division can be considered a practical means for making large area, sub 100 nm period gratings.

An alternative to x-ray spatial-period-division is to use deep UV radiation. With an ArF laser (193 nm), for example, the parent mask can be an aluminum grating on quartz. We have demonstrated spatial-period-division (i.e., "doubling" a 199 nm period aluminum grating into a 99.5 nm period grating in PMMA) with such a configuration and will report on it fully in the near future.

ACKNOWLEDGEMENTS

The authors are grateful to J. M. Carter for his expert technical assistance, D. C. Flanders for his contributions to the early spatial-period-division work, M. Griswold for electron microscopy, G. Stone, M. Roth and G. Howe for assistance with the imaging spectrometer, and D. Ciarlo for fabricating the gold grid pattern used for the free-standing gratings. R. M. Osgood and D. J. Erlich collaborated on the UV spatial-period-division.

REFERENCES

1. D. C. Flanders, A. M. Hawryluk and H. I. Smith, *J. Vac. Sci. Technology*, 16 1949 (1979).
2. A. M. Hawryluk, Ph.D. Thesis, Massachusetts Institute of Technology, 1981.
3. D. P. Kern and D. A. Nelson, *Proc. of Symposium on Electron and Ion Beam Science and Technology, Ninth International Conference*, p. 489, May 1980, R. Bakish, editor, *1980, Electrochemical Society.
4. H. J. Hagemann, W. Gudst, C. Kunz, *J. Opt. Soc. Am.*, 65, 742, (1975).
5. D. E. Bean, *IEEE Trans, Electron Devices*, ED-25, 1185 (1978).
6. D. C. Flanders, *J. Vac. Sci. Technology*, 16, 1615 (1979).
7. R. H. Price, *AIP Proceedings of Topical Conference on Low Energy X-ray Diagnostics*, June, 1981, Monterey, California, D. T. Attwood, editor.
8. D. C. Flanders and H. I. Smith, *J. Vac. Sci. Technology*, 15, 995 (1978).
9. E. T. Arakawa, P. J. Caldwell and M. W. Williams, "Soft X-ray Transmission Gratings", *Periodic Structures, Gratings, Moire Patterns and Diffraction Phenomena, Proc. of S.P.I.E.*, 240, p. 52, July 29-Aug. 1, 1980, San Diego, California, C.H. Chi, E. G. Loewen, C. L. O'Bryan, editors, *1981, S.P.I.E.

FIGURE CAPTIONS

Fig. 1 An SEM micrograph of an x-ray mask consisting of an $0.3 \mu\text{m}$ period grating in 70 nm thick gold on polyimide. This grating was produced by holographic lithography and ion beam etching.

Fig. 2 (a) An SEM micrograph of an $0.3 \mu\text{m}$ period grating in PMMA, 0.7 μm thick, on a gold plating base, produced by x-ray lithography.
(b) SEM micrograph of a gold grating produced by electroplating into the openings of the PMMA grating in (a).

Fig. 3 SEM micrograph of a 199 nm period grating with 40 nm wide "slits" in 180 nm thick gold; (a) cleaved edge view, (b) top view. This grating is similar to gratings made in 250 nm thick gold that were used for spatial-period-division at $\lambda = 4.5 \text{ nm}$.

Fig. 4 Schematic diagram of the imaging spectrometer. A gold aperture mask was back-lit by the radiation emitted from a tungsten anode. The 22x Wolter microscope focuses the transmitted x-rays onto an image plane after first passing through the grating. The diffraction pattern is recorded on film.

Fig. 5 Diffraction pattern showing the M_α , M_β , and M_γ lines of the tungsten anode. A microdensitometer trace of this figure indicates a $\lambda/\Delta\lambda$ of 200 at $\lambda = 0.69$ nm.

Fig. 6 SEM micrograph of the cleaved edge. (a), and top view, (b), of a 99.5 nm period grating exposed in 150 nm thick PMMA by x-ray spatial-period-division. The dip, which extends about 20 nm into the top of each PMMA line, is a higher-spatial-frequency interference effect.



1 μ m

Fig. 1



Fig. 2(a)



1 μm

Fig. 2(b)

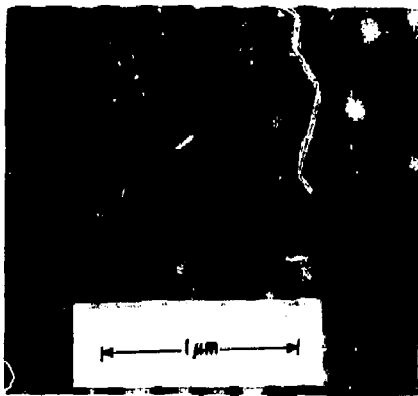
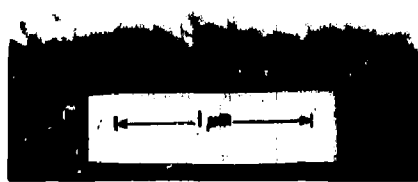


Fig. 3

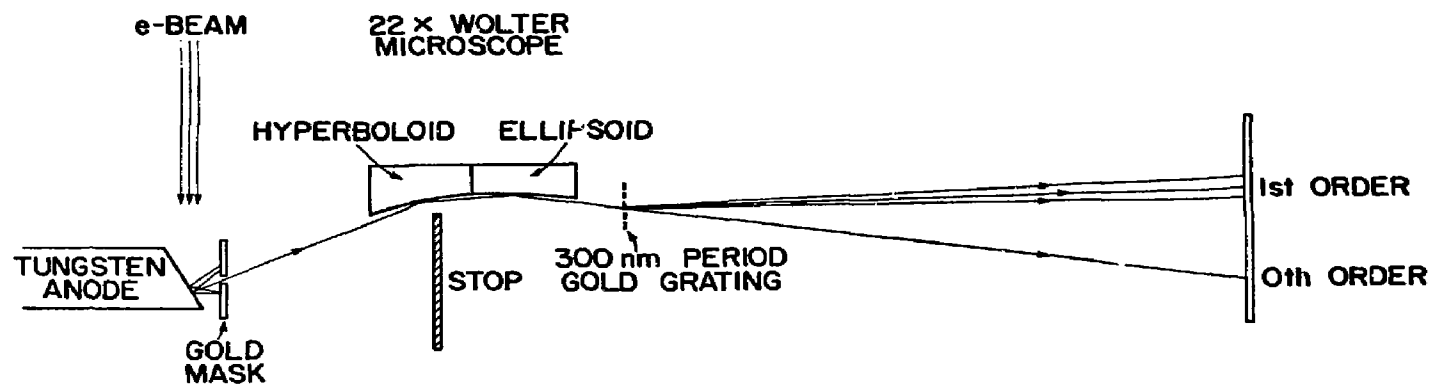


Fig. 4

FIRST ORDER

— TUNGSTEN M_a (6.98 Å)
— TUNGSTEN M_b (6.76 Å)
— TUNGSTEN M_c (6.09 Å)

ZEROTH ORDER

Fig. 5



→ ←
995 Å



→ ←
995 Å

Fig. 6